PLA/Lignocellulosic Fiber Composites: Particle Characteristics, Interfacial Adhesion, and Failure Mechanism

Gábor Faludi,[1,2] **Gábor Dora,**[1,2] **Balázs Imre,**[1,2] **Károly Renner,**[1,2] **János Móczó,**[1,2] **Béla Pukánszky**[1,2]

[1]Laboratory of Plastics and Rubber Technology, Budapest University of Technology and Economics, H-1521 Budapest, Hungary
[2]Institute of Materials and Environmental Chemistry, Chemical Research Center, Hungarian Academy of Sciences, H-1525 Budapest, Hungary
Correspondence to: J. Móczó (E-mail: jmoczo@mail.bme.hu)

ABSTRACT: Poly(lactic acid) (PLA) composites were prepared using six lignocellulosic fibers with widely varying particle characteristics. The composites were characterized by tensile testing, scanning electron (SEM), and polarization optical microscopy (POM). Micromechanical deformation processes during loading were followed by acoustic emission measurements. Interfacial adhesion was estimated by three independent methods. Contrary to most claims published in the literature, interfacial adhesion between PLA and natural fibers was found to be rather strong, a result confirmed by the quantitative estimation of adhesion strength, acoustic emission measurements, and SEM study. Strong interfacial adhesion results in weak dependence of the extent of reinforcement on the particle characteristics of the reinforcing fibers. Both acoustic emission measurements and microscopy indicated that the dominating micromechanical deformation process is the fracture of the fibers and close correlation was found between the initiation stress of fiber fracture, reinforcement, and the ultimate strength of the composites. © 2013 Wiley Periodicals, Inc. J. Appl. Polym. Sci. **2014**, *131*, 39902.

INTRODUCTION

The interest in using polymeric materials derived from renewable resources increases by the day because of the considerably improved environmental conscientiousness of the society and the fear from the depletion of petrochemical based plastics.[1] Poly(lactic acid) (PLA) seems to be the polymer which exploits the most successfully this surge of demand for such materials and satisfies the requirements of large scale processing and application at the same time. PLA has several advantages, among others it can be produced from renewable resources[2] thus its application does not generate supplementary CO_2 emission,[3] it is recyclable and compostable, it has good stiffness and strength, and its properties can be modified and adjusted to a large number of applications in various ways.[4,5] On the other hand, this polymer has some drawbacks as well, including moisture sensitivity, fast physical ageing, poor impact resistance, and relatively high price.[4,5] As a consequence, many attempts are made to modify it by plasticization,[6–8] copolymerization,[9–11] blending,[12,13] or by the production of particulate filled or fiber reinforced composites.[14–18]

In the last decade, many attempts were made to modify PLA with inorganic fillers or natural reinforcements. The structure of these latter materials is heterogeneous; it contains various phases and possesses one or more interfaces. Several factors determine the properties of such materials; one of the most important is interfacial adhesion. The question of interfacial adhesion was mentioned or expressively discussed in several articles, but the conclusions drawn are rather contradictory. The inorganic fillers studied included hydroxyapatite fibers or particles,[18,19] titanium dioxide,[20,21] zeolite,[22] calcium phosphate[15] and sulphate,[23] calcium carbonate,[14,24] layered silicates,[25–27] expanded graphite,[28,29] graphene nanosheets,[30] carbon nanotubes[31,32] and some other fillers or reinforcements.[33,34] Both weak and strong adhesion was found in these composites depending on the type of filler, surface modification, method of determination etc., but the number of composites with good interfacial adhesion was more than twice as many[18,19,21,23,27–31] as those with weak interaction.[14,15,20,25,26] These results indicate at least that PLA is capable of forming strong interaction with solid surfaces.

The picture becomes even more complicated when lignocellulosic fibers are used for reinforcement. The observations are occasionally contradictory even within the same article. Plackett[35] for example observed the increase of strength in PLA containing 40 wt % jute fabric compared with that of the neat matrix and explained it with good adhesion. On the other hand, he found

voids around the fibers on SEM micrographs and concluded that adhesion must be improved. Similarly, Huda et al.[36] deduced from the analysis of stiffness that interfacial adhesion is weak, but based on SEM micrographs they reasoned that adhesion must be strong, since no debonding was observed on the matrix/fiber interface and that failure was caused by matrix fracture. However, the analysis of articles available for us showed that based on their results most authors arrived to the conclusion that the interaction between PLA and lignocellulosic fibers is weak.[16,35–40]

It must be considered here, however, that this conclusion was drawn mainly from the results of tensile tests[35,37,38,40–42] and from SEM micrographs.[16,35–39,41–44] It was shown earlier that several micromechanical deformation processes take place during the deformation and failure of polymer/wood composites. These processes are competitive and they can often proceed also simultaneously. It is not very surprising therefore that micrographs taken from fracture surfaces are complex and difficult to interpret. Void formation indicating debonding, pull-out, and also fiber fracture are often observed simultaneously on them. The first two processes are easier to observe and interpret thus the conclusion that weak interaction develops between the components is almost evident. Similarly complicated is the interpretation of the composition dependence of tensile yield stress or tensile strength. Weak interfacial adhesion is often deduced from the fact that these mechanical properties decrease with increasing amount of the lignocellulosic fibers. One must keep in mind, however, that besides adhesion the extent of reinforcement depends also on other factors like matrix properties, aspect ratio, and orientation. The composition dependence of strength cannot be interpreted without the consideration of these factors.

In the frame of a large project on PLA/wood composites some particular questions have been already addressed. In our former study,[45] it was shown that the structure of the filler influences the properties of the composites and reinforcement depends on interfacial adhesion. In another particular study[46] on PLA composites reinforced with a fiber having large aspect ratio the structural analysis indicated formation of a network purely from geometrical reasons. Considering all apparent or real contradictions as well as the importance of interfacial interactions in the determination of composite properties, the main goal of this study was the estimation of the strength of adhesion between lignocellulosic fibers and PLA. To achieve this goal, composites were prepared with six different reinforcements of widely varying chemical composition and particle characteristics. An attempt was made to determine the failure mechanism of the composites, a question rarely discussed in literature. Finally, the practical consequence of adhesion and deformation mechanism is discussed in the final section of the article.

EXPERIMENTAL

The PLA used in the experiments was obtained from Nature-Works (USA). The selected grade (Ingeo 4032D, $M_n = 88500$ g/mol and $M_w/M_n = 1.8$) is recommended for extrusion. The polymer (<2% D isomer) has a density of 1.24 g/cm^3, while its MFI is 3.9 g/10 min at 190°C and 2.16 kg load. Six commercially available lignocellulosic fibers were used as reinforcements without any further treatment in the study: four wood fibers, microcrystalline cellulose, and the heavy fraction of grinded corn cob. Because of their importance particle characteristics of the fibers were characterized quite thoroughly. The SEM micrographs presented in Figure 1 show the fillers used. Particle size and aspect ratio change in a wide range. Particle characteristics were determined quantitatively by laser light scattering, but also by image analysis of SEM micrographs. The results are compiled in Table I. Since in an earlier study it was found that aspect ratio is one of the most important characteristics determining composite properties, this information was included into the abbreviation of the fibers in order to facilitate discussion. The letters indicate the origin of the fibers, while the numbers correspond to 10 times the aspect ratio (see Table I).

Both PLA and the fibers were dried in a vacuum oven before composite preparation (110°C for 4 h and 105°C for 4 h, respectively). The components were homogenized using a Brabender W 50 EHT internal mixer at 180°C, 50 rpm for 10 min. Wood content changed in a relative wide range, composites contained 5, 10, 15, 20, 30, 40, 50, and 60 vol % lignocellulosic fibers. The homogenized material was compression molded into 1-mm thick plates at 190°C using a Fontijne SRA 100 machine. All specimens were kept in a room with controlled temperature and humidity (23°C and 50%) for at least one week prior further testing.

Mechanical properties were characterized by the tensile testing of specimens cut from the 1-mm thick plates using an Instron 5566 apparatus. The measurements were done at 5 mm/min cross-head speed and 115-mm gauge length. Micromechanical deformation processes were followed by acoustic emission (AE) measurements. A Sensophone AED 40/4 apparatus was used to record and analyze acoustic signals during tensile tests. The particle characteristics of wood and the structure, as well as the deformation mechanism of the composites were studied by scanning electron microscopy, SEM (JEOL JSM-6380 LA). Micrographs were recorded on tensile fracture surfaces. Failure mechanism was studied also on model composites by polarization optical microscopy (POM). Thin (about 150 μm) films were compression molded from the composites, fractured by tensile testing and the broken halves were studied in the microscope to determine failure mode.

RESULTS AND DISCUSSION

The morphology of PLA/lignocellulosic composites can be relatively complicated. The polymer can crystallize, but the rate of crystallization is rather slow thus under the conditions of normal processing operations it remains mostly amorphous; its crystalline content is very small. Besides crystalline structure, the distribution of the fibers in the matrix, i.e., the possible formation of aggregates, especially at large fiber loadings, is also an important issue. The fiber might influence also interphase formation and the mobility of the polymer molecules. These questions were investigated in a previous study in detail.[47] It was found that crystallinity is negligible in PLA, while in PP/wood
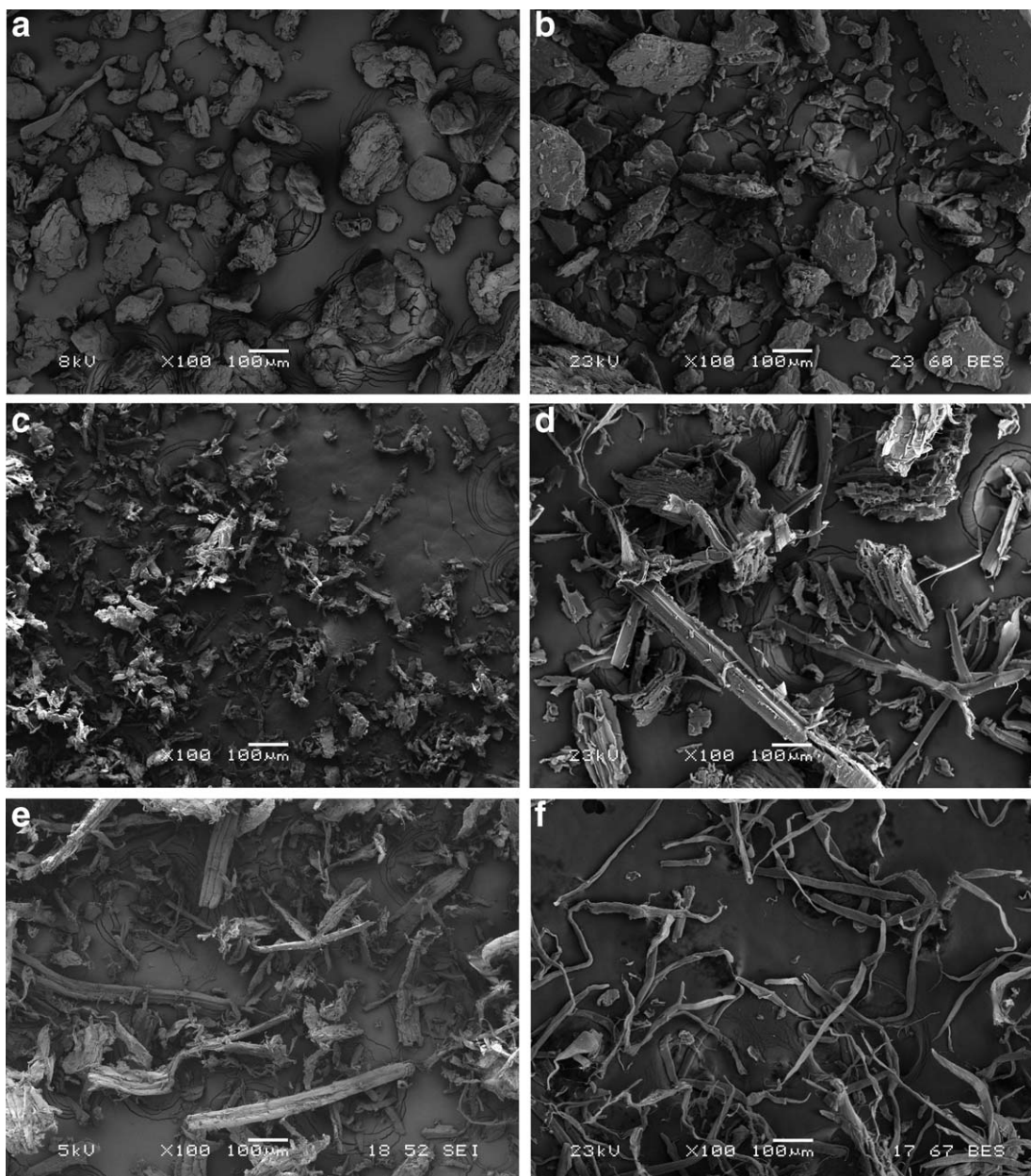
Figure 1. Particle characteristics of the studied lignocellulosic fibers (SEM micrographs); (a) corn cob (CC23), (b) Vivapur MCC (MC29), (c) Arbocel CW 630 (W35), (d) Lasole 200/150 (W54), (e) Filtracel EFC 1000 (W68), and (f) Arbocel FT 400 (W126).

Table I. Particle Characteristics of the Studied Lignocellulosic Fibers

Fiber	Abbreviation	D[4,3][a] (μm)	Length[b] (μm)	Diameter[b] (μm)	Aspect ratio[b]
Corn cob	CC23	143.4	108.1	55.7	2.3
Vivapur MCC	MC29	138.0	85.0	30.5	2.9
Arbocel CW 630	W35	39.6	93.5	33.3	3.5
Lasole 200/150	W54	280.8	167.9	41.4	5.4
Filtracel EFC 1000	W68	213.1	363.4	63.9	6.8
Arbocel FT 400	W126	171.2	235.2	21.8	12.6

[a] Volume average particle size.
[b] Average values determined from scanning electron micrographs.
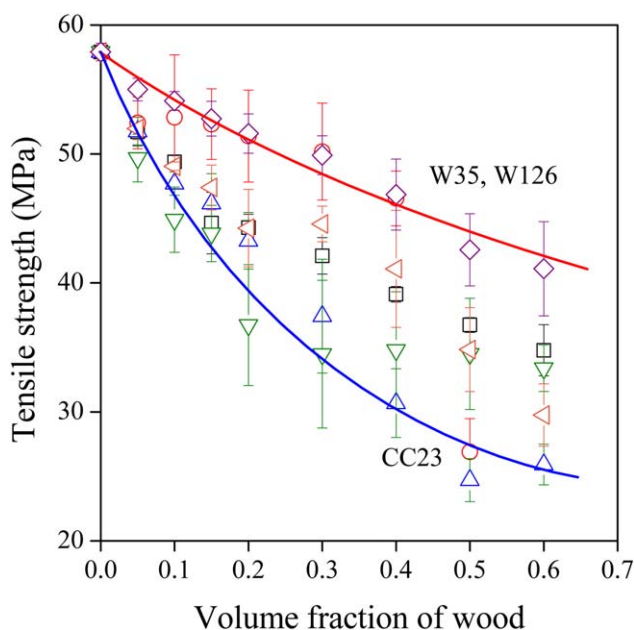
Figure 2. Effect of the type and amount of reinforcement on the tensile strength of PLA/lignocellulosic fiber composites. Symbols: (Δ) CC23, ($\triangledown$) MC29, ($\diamond$) W35, ($\triangleleft$) W54, ($\square$) W68, ($\bigcirc$) W126. [Color figure can be viewed in the online issue, which is available at wileyonlinelibrary.com.]

composites limited aggregation resulted from the mere physical contact of the particles due to geometrical reasons.[48] As a consequence we refrain from the detailed discussion of structure and focus mostly on properties, micromechanical deformations, interfacial adhesion, and deformation and failure mechanism. Consequences for practice are discussed in the final section of the article.

Properties, Reinforcement

The properties of the composites change with fiber content according to the expectations and in agreement with literature references. Stiffness increases from 3.4 GPa of the matrix to about 7 GPa of the composite with the largest fiber content (not shown). The effect of particle characteristics is slight, only the composite containing the fiber with the largest aspect ratio (W126) has distinctly larger stiffness than the rest of the composites. Structural effects are not reflected by the composition dependence of stiffness, a small extent of aggregation might be detected at the largest wood content at most.

The characteristics of the reinforcement influence tensile strength much more significantly, as shown in Figure 2. Tensile strength decreases with increasing fiber content for all reinforcements, but the decrease is relatively moderate for the thin long fibers (W126) and for the wood having the smallest particle size (W35, 40 μm). Composites prepared from corn cob have the smallest strength and the rest of the composites are located between these two boundary cases. The results indicate that both aspect ratio and particle size influence composite strength, and large reinforcement can be achieved with large aspect ratio and small size.

From the decrease of strength with increasing fiber content, several groups deduced that interfacial adhesion is weak in PLA/

wood composites.[36–38,40,41] This conclusion can be further supported by the comparison of PLA composites with PP/wood composites. Adhesion is poor between PP and wood and without a coupling agent, composite strength decreases with increasing fiber content. On the other hand, if a coupling agent like maleated polypropylene (MAPP) was added to the composite, strength increased considerably with fiber content, i.e., from about 17 MPa to 41 MPa in a PP random copolymer.[49] It must be considered here, however, that reinforcement depends also on the properties of the matrix; it decreases with increasing matrix stiffness and strength. The PP mentioned above had a strength of 17 MPa, while the strength of our PLA is close to 60 MPa. As a consequence, the strength of interfacial adhesion cannot be deduced directly from such a comparison of different materials or from the composition dependence of mechanical properties.

On the other hand, the extent of reinforcement can be estimated quantitatively with the help of simple models. The dependence of tensile strength on filler content can be expressed as[50]

$$\sigma_T = \sigma_{T0} \lambda^n \frac{1-\varphi}{1+2.5\varphi} \exp(B\varphi) \qquad (1)$$

where σ_T and σ_{T0} are the true tensile strength of the composite and the matrix, respectively ($\sigma_T = \sigma\lambda$ and $\lambda = L/L_0$), λ is relative elongation ($\lambda = L/L_0$, where L_0 is gauge length and L the length measured at the moment of failure), n is a parameter expressing the strain hardening tendency of the matrix, φ is the volume fraction of the fiber and B is related to its relative load-bearing capacity, i.e., to the extent of reinforcement, which depends among other factors also on interfacial interaction. Equation (1) can be written in linear form

$$\ln \sigma_{Tred} = \ln \frac{\sigma_T(1+2.5\varphi)}{\lambda^n(1-\varphi)} = \ln \sigma_{T0} + B\varphi \qquad (2)$$

and the plot of the natural logarithm of reduced tensile strength against fiber content should result in a linear correlation, the slope of which is proportional to the load-bearing capacity of the reinforcement and under certain conditions to the strength of interaction. In Figure 3, the strength of three series of composites is plotted against filler content in the form indicated by eq. (2). Linear correlations with different slopes were obtained indeed indicating dissimilar reinforcing effect of the fibers. The fibers were selected to show the extremes of reinforcement and an additional fiber for comparison. Rather surprisingly the reinforcement achieved by the six fibers differs from each other only very little. If PP is used as comparison again, changing adhesion resulted in an increase from 1.1 to 5.3 there,[51] while B values change from 1.7 to 2.6 in the PLA matrix. The extent of reinforcement is shown quantitatively for all composites in Table II. If the values are compared with the particle characteristics listed in Table I it can be seen that small aspect ratio results in small reinforcement (CC23, AR = 2.3), while small size (W35, 40 μm) and large aspect ratio (W126, AR = 12.6) leads to stronger reinforcement. The small differences and the limited effect of particle characteristics on reinforcement are
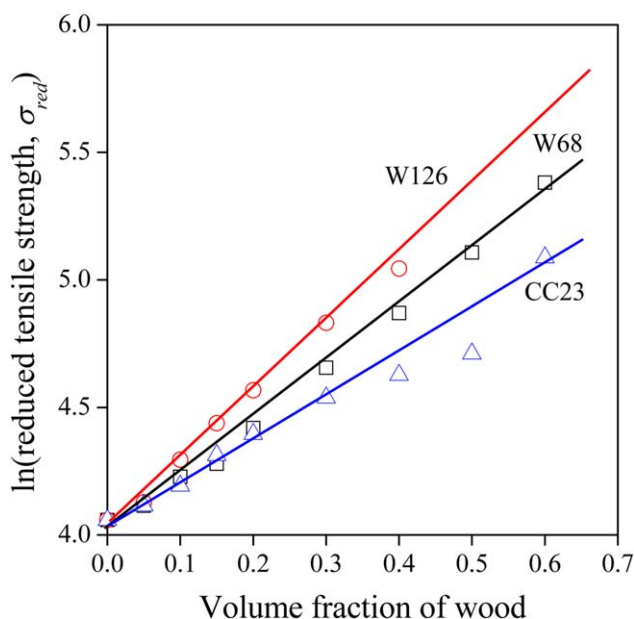
Figure 3. Reduced tensile strength of selected composites plotted against fiber content according to eq. (2). Symbols are the same as in Figure 2. [Color figure can be viewed in the online issue, which is available at wileyonlinelibrary.com.]
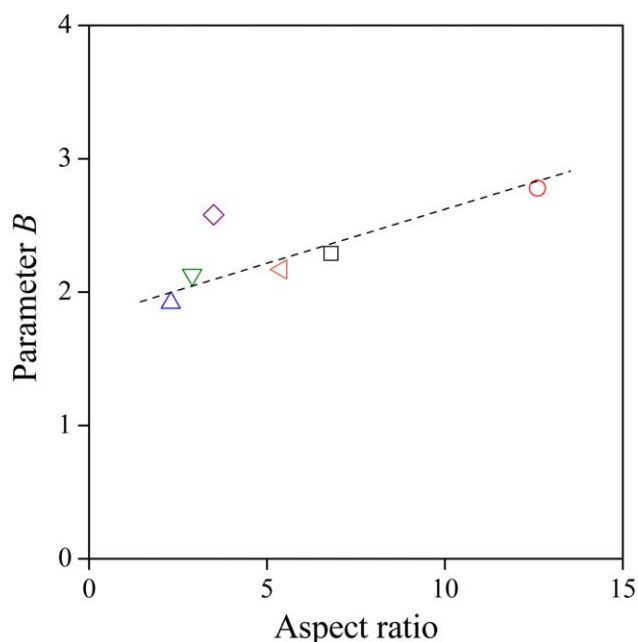

Figure 4. Correlation between the aspect ratio of the lignocellulosic fibers used and their reinforcing effect (Parameter B). Symbols are the same as in Figure 2. [Color figure can be viewed in the online issue, which is available at wileyonlinelibrary.com.]

quite surprising. This observation is further supported by Figure 4 in which parameter B expressing reinforcement is plotted against the aspect ratio of the fibers. This characteristic had the most pronounced effect on reinforcement in PP/wood composites,[51] but the effect depended also on adhesion; it was much weaker at good than at poor adhesion. One might deduce from this comparison that interfacial adhesion might be stronger in PLA/wood composites than indicated in a large number of publications.[16,36–38,40,41]

Micromechanical Deformations

Because of the dissimilar elastic properties of the matrix polymer and the inclusion, stress concentration develops around this latter in heterogeneous polymers. Local stress maxima initiate local deformation processes some of which are accompanied by acoustic events. Sound waves can be picked up by microphones and the analysis of the signals may yield valuable information about the deformation and failure of the material. The result of an acoustic measurement carried out on a PLA/wood

composite is presented in Figure 5. Each small circle is an acoustic event the amplitude of which can be deduced from the right hand axis of the graph. The corresponding stress vs. strain trace is also shown as reference. It can be seen that significant acoustic activity starts above a certain deformation and that amplitudes cover a wide range. Further conclusion is difficult to deduce from individual signals, additional analysis is needed to
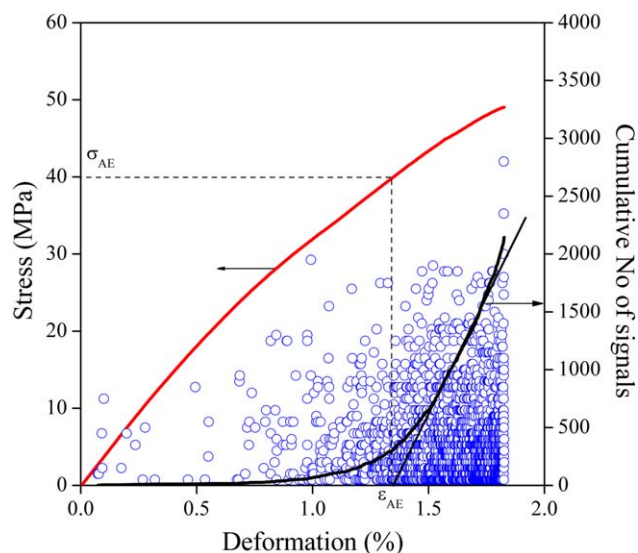
Table II. Reinforcing Effect of the Studied Lignocellulosic Fibers in PLA

Fiber	Matrix strength[a] (MPa)	Parameter B	R^{2b}
CC23	58.2	1.73	0.9978
MC29	54.2	2.17	0.9854
W35	60.1	2.44	0.9987
W54	58.3	2.05	0.9922
W68	55.9	2.23	0.9944
W126	58.4	2.56	0.9958

[a] Calculated from the intersection of the $\ln\sigma_{red}$ vs. φ lines (measured value 57.9 MPa).
[b] Determination coefficient showing the goodness of the linear fit.

Figure 5. Acoustic emission testing of a PLA composite containing 10 vol % (W68) wood. Small circles indicate individual acoustic events. Stress vs. strain and cumulative number of signal vs. strain traces. [Color figure can be viewed in the online issue, which is available at wileyonlinelibrary.com.]
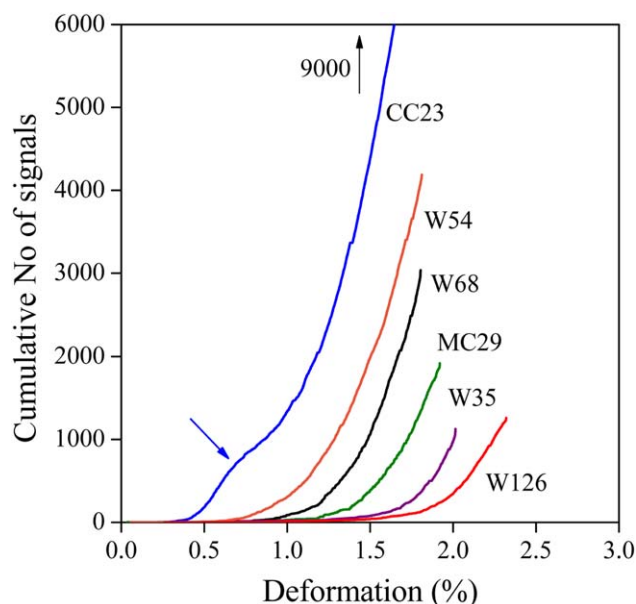
Figure 6. Comparison of the cumulative number of signal traces for all PLA/lignocellulosic fiber composites at 10 vol % fiber content. [Color figure can be viewed in the online issue, which is available at wileyonlinelibrary.com.]

Figure 7. Dependence of the initiation stress of the dominating micromechanical deformation process on wood content. Symbols are the same as in Figure 2. [Color figure can be viewed in the online issue, which is available at wileyonlinelibrary.com.]

extract more information from the results. The cumulative number of signals is also plotted as a function of deformation in Figure 5 together with the stress vs. strain trace. It can be seen that acoustic activity increases continuously until the failure of the composite. Characteristic deformation and stress values related to the initiation of the dominating micromechanical deformation mechanism can be determined as indicated in Figure 5.

Cumulative number of signal traces are plotted for all composites containing the various fibers in 10 vol % in Figure 6. The traces are very similar to each other; they differ only in the total number of signals detected until failure, and in initiation deformation. The trace recorded on the composite containing corn cob shows an additional difference, it has a shoulder (shown by an arrow) at small elongations indicating the occurrence of an additional deformation process. The shape of the cumulative number of signal vs. elongation traces could be related to the mechanism of deformation earlier.[49,51,52] Traces similar to those shown in Figure 6 were obtained on composites with strong interfacial adhesion in which fiber fracture was the dominating mechanism. In the case of particulate filled composites, in which debonding is the only deformation process, step-like traces approaching a plateau value were recorded in all matrices including PLA.[53,54] The shape of the traces indicates stronger PLA/fiber adhesion than claimed by literature references.

Characteristic stresses derived from the cumulative number of signal vs. deformation and the corresponding stress vs. deformation traces are plotted in Figure 7 for all composites. According to the two steps, two characteristic values were determined for corn cob indicated by empty (first step) and full (second step) symbols in the figure. The composites can be divided into three groups. Probably not very surprisingly, the wood with small
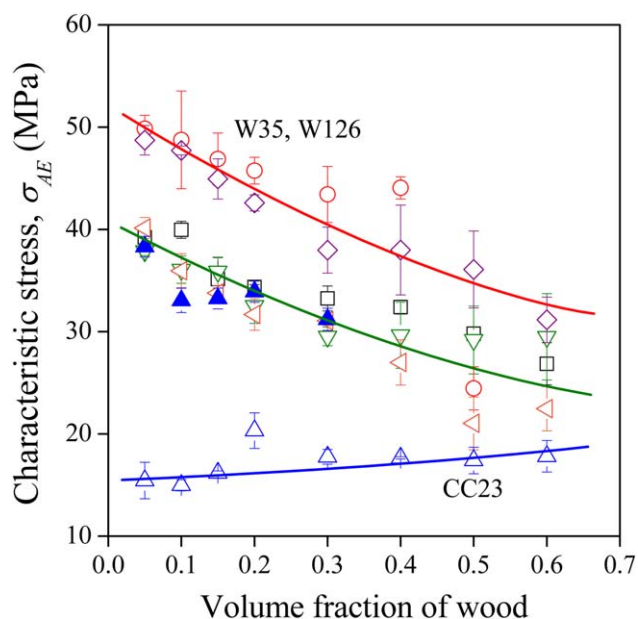
particle size (W35) and the one having large aspect ratio (W126) forms one group with the largest characteristic stress, while corn cob forms a group of its own. The rest of the fibers behave very similarly. These results clearly prove that the dominating micromechanical deformation process occurring during the deformation of PLA/wood composites depend on the particle characteristics of the reinforcement. In Figure 8, the
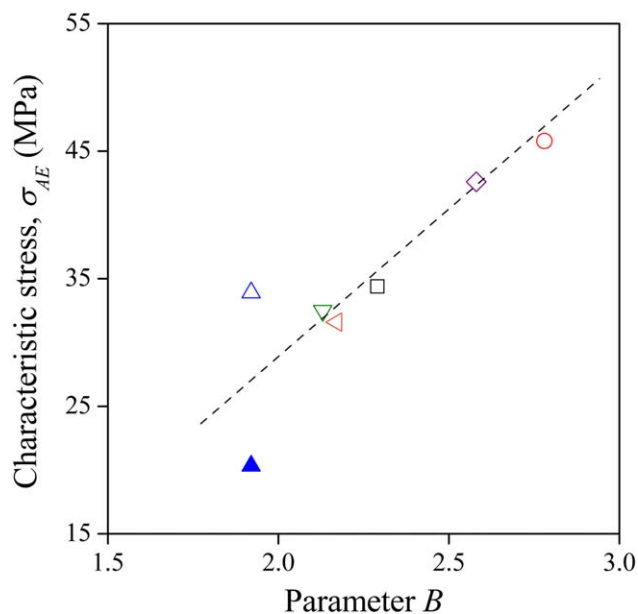

Figure 8. Correlation between the characteristic stress determined by acoustic emission measurement and the reinforcing effect of the fibers in PLA/wood composites. Symbols are the same as in Figure 2. [Color figure can be viewed in the online issue, which is available at wileyonlinelibrary.com.]

characteristic stress derived from acoustic emission measurements at 20 vol % fiber content is plotted against the extent of reinforcement determined from tensile strength. Apart from the value for corn cob, the correlation is extremely close indicating that macroscopic composite properties depend very much on the micromechanical process taking place in the composite during deformation. The behavior of corn cob must be studied more in detail in the future.

Interfacial Adhesion
In particulate filled and especially in short fiber reinforced composites the direct determination of interfacial adhesion is difficult. It was mentioned earlier that conclusions drawn from the analysis of SEM micrographs are very uncertain because a number of processes can take place simultaneously (debonding, fiber pull-out, fiber fracture), because of the limited area studied, and because SEM cannot supply quantitative values for adhesion anyway. The other frequently used approach, the composition dependence of tensile strength can be also misleading because of the simultaneous effect of several factors (matrix properties, adhesion, orientation, aspect ratio).

Different approaches can be used for the estimation of interfacial adhesion in particulate filled polymers. The first is based on surface energy and the calculation of the reversible work of adhesion

$$W_{AB} = 2\left(\gamma_1^d \gamma_2^d\right)^{1/2} + 2\left(\gamma_1^p \gamma_2^p\right)^{1/2} \quad (3)$$

where γ_1^d and γ_2^d are the dispersion, while γ_1^p and γ_2^p the polar components of surface tension for components 1 and 2, respectively. The more accurate approach of using acid–base interactions for the determination of the reversible work of adhesion cannot be used in our composites because the number of interacting acid–base sites located on the surface is not known but it is necessary for the calculation.[55] The reversible work of adhesion was shown to correlate closely with reinforcement.[56] Another approach for the estimation of the strength of interfacial adhesion is based on the determination of debonding stress by acoustic emission measurements.[57] Debonding stress is defined as[58]

$$\sigma^D = -C_1 \sigma^T + C_2 \left(\frac{E W_{AB}}{R}\right)^{1/2} \quad (4)$$

where σ^D and σ^T are debonding and thermal stresses, respectively, E the Young's modulus of the matrix, W_{AB} the reversible work of adhesion, R the radius of the particles, while C_1 and C_2 are geometric constants related to the debonding process. If the parameters of the equation are known, which were calculated from measurements done on polymer/filler pairs with known characteristics (E, R, W_{AB}), the stiffness of the matrix and the size of the particles, which is usually known, the strength of adhesion can be calculated. The term F_a is used here instead of W_{AB} in subsequent discussions to differentiate the approach of determination. Finally, the strength of interfacial adhesion can be also estimated from the composition dependence of composite strength with the model presented above [see eq. (1)], if the dominating deformation mechanism is debonding.

Table III. Estimation of the Strength of Interfacial Adhesion in PLA/Wood Composites by Various Approaches; the Same Reinforcement (Corn Cob) Was Used in All Three Matrices

Matrix	Approach		
	Work of adhesion (mJ/m^2)	Debonding (mJ/m^2)	Parameter B
PP	82.2	67	1.16
PLA	97.7	93	1.73
PVC	95.6	162	2.59

Unfortunately, all three approaches can be used only with serious limitations in our PLA/wood composites. Equation (3) does not estimate specific interactions very accurately, although the formation of such was expected between the carbonyl groups of PLA and the hydroxyl groups of cellulose. The approach expressed in eq. (4) assumes spherical particles and debonding as the dominating process and neither is fulfilled in our case. Finally, failure mechanism and particle shape are important factors also in the third approach; parameter B offers information about reinforcement, but the estimation of interfacial adhesion is questionable. Nevertheless, in lack of better solution all three approaches were applied to our composites and the results are compiled in Table III. Similar calculations were carried out also for PP/wood and PVC/wood composites to facilitate interpretation. It can be seen that all three approaches indicate stronger adhesion in PLA/wood than in PP/wood composites. Surprisingly, the strongest adhesion develops in PVC composites. The same filler, corn cob, was used as reinforcement in all three matrices. In spite of their serious limitations and uncertainty, none of the approaches indicate weak, but at least intermediate interaction in PLA/wood composites. We should like to remind the reader here that debonding and pull-out are the dominating micromechanical deformation processes in PP/wood composites when adhesion is poor and fiber fracture occurs at good adhesion.[51] As a consequence, any one of them or both can be expected in our PLA/wood composites.

An additional attempt was made to estimate the level of adhesion and to compare different polymer/wood composites. As mentioned before, the value of parameter B, i.e., reinforcement depends also on the properties of the matrix [see Eq. (2)]. To compensate for this effect, parameter B was weighed with the yield stress of the matrix and plotted this corrected value, B_c, against matrix yield stress in Figure 9. Values obtained for CaCO$_3$ composites prepared with different matrices are also plotted as comparison. It can be seen that the values are very similar for the latter, almost independently of the matrix polymer. Two groups can be distinguished in the case of wood composites. The values obtained at poor adhesion in PP are significantly smaller than in any of the other cases, which are similar for PP homopolymer and random copolymer at good adhesion, PVC and PLA. Variation within a group of the same matrix is caused by the effect of other factors influencing reinforcement, i.e., aspect ratio, orientation, particle size etc. The conclusion must be drawn that adhesion is very similar in these composites and it is known that it is strong in PP composites containing a MAPP coupling
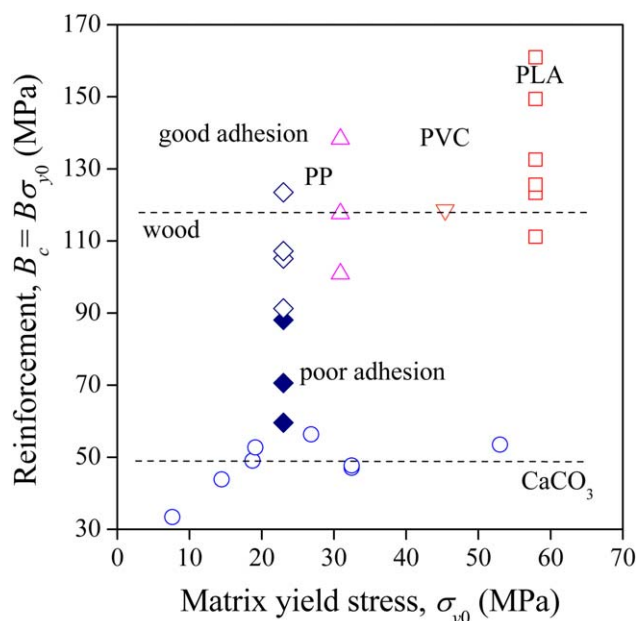
Figure 9. Comparison of interfacial adhesion in various polymer/wood composites. Corrected parameter B_c ($B\sigma_{y0}$) plotted against the yield stress of the matrix (σ_{y0}). Symbols: (○) CaCO₃ composites, (◆) PP random copolymer, poor adhesion, (◇) random copolymer, good adhesion, (△) PP homopolymer, good adhesion, (▽) PVC, (□) PLA. [Color figure can be viewed in the online issue, which is available at wileyonlinelibrary.com.]

agent. Practically all evidence indicates that contrary to claims published in the literature interfacial adhesion is not weak in PLA/wood composites, but considerable specific interactions develop between the components.

Failure Mechanism, Consequence

Based on the considerations presented above, we came to the final conclusion that adhesion is relatively strong between ligno-cellulosic fibers and the PLA matrix. Moreover, the shape of the cumulative number of signal vs. deformation traces differed from that observed in cases when debonding was the dominat-ing micromechanical deformation process.[49,51,53,59] SEM micro-graphs were prepared to reveal or at least supply some
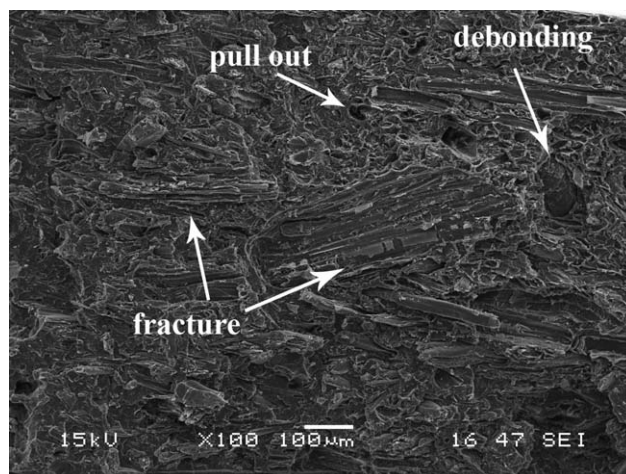

Figure 10. SEM micrograph taken from the fracture surface of a PLA/wood (W68) composite at 20 vol % wood content. Fracture surface was created at failure in the tensile test.

additional information about the mechanism of failure in our PLA/wood composites. Figure 10 shows such a micrograph which is typical for most of the composites studied. The domi-nating process is definitely fiber fracture with a limited number of debonding and fiber pull-out events. However, the number of these latter is much smaller than that of fiber fracture. This observation agrees quite well with the fact that very similar cumulative number of signal vs. deformation traces were obtained in PP/wood composites with good adhesion[49,52] as those shown in Figure 6. The fact of fiber fracture was strongly supported and verified also by the POM study. Selected micro-graphs are shown in Figure 11. In composites containing large particles oriented perpendicularly to the direction of the load, always the fiber fractures leading to the failure of the composite itself. Failure might be different for small and/or thin fibers, like W35 and W126. The only lignocellulosic filler which behaved differently was corn cob. Extensive particle fracture could be observed in this material as well (see Figure 12a), but the presence of other mechanisms was also detected. As Figure 12b shows certain particles debond from the matrix forming voids around them. Either this mechanism or the fracture of
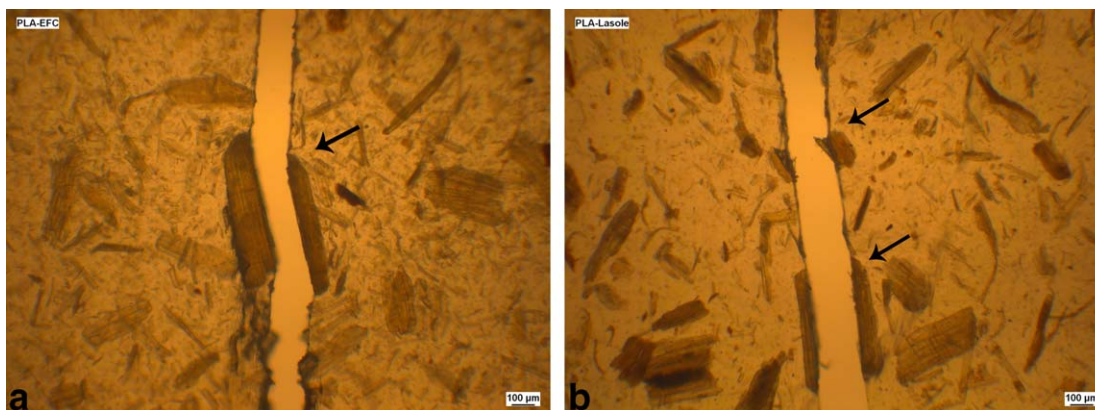

Figure 11. Fiber fracture in PLA model composites, POM micrographs. (a) W68, (b) W54. The composites contained 10 vol % fiber. [Color figure can be viewed in the online issue, which is available at wileyonlinelibrary.com.]
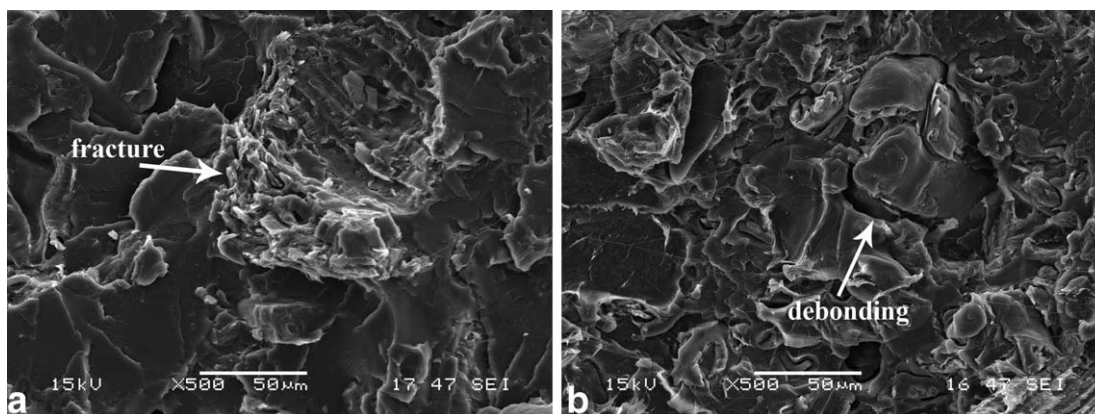
Figure 12. Competitive micromechanical deformation processes in PLA/corn cob (20 vol %) composites. (a) fiber fracture, (b) debonding.

weaker particles may result in the shoulder appearing on the cumulative number of signal vs. deformation trace of composites containing corn cob in Figure 6. The phenomenon needs further measurements and study.

Finally, the influence of the dominating micromechanical deformation process on the macroscopic properties and performance of the composites must be discussed. Composite strength is plotted against the characteristic stress determined by acoustic emission in Figure 13. Extremely close correlation exists between the two quantities indicating that processes occurring around the particles determine the performance of the composite. The similar values also show that the fracture of wood particles leads to the catastrophic failure of the composite thus further improvement in composite properties is possible only by the increase of the inherent strength of wood or in a limited

extent by the proper selection of the particle characteristics of the reinforcement (see W35 and W126).

CONCLUSIONS

The study of deformation and failure mechanisms as well as interfacial interactions in PLA/lignocellulosic fiber composites indicated that contrary to most claims published in the literature, interfacial adhesion is rather strong between PLA and natural fibers. This conclusion was confirmed by three independent approaches used for the quantitative estimation of the strength of interfacial interactions, by acoustic emission measurements and by SEM study. Strong interfacial adhesion results in weak dependence of the extent of reinforcement on the particle characteristics of the reinforcing fibers. Both acoustic emission measurements and microscopy indicated that the dominating micromechanical deformation mechanism is the fracture of the fibers and close correlation was found between the initiation stress of fiber fracture, reinforcement, and ultimate composite strength. Corn cob behaved differently from the rest of the reinforcements used, at least two consecutive deformations were detected during the loading of its composites. Further study is needed to identify these unambiguously.
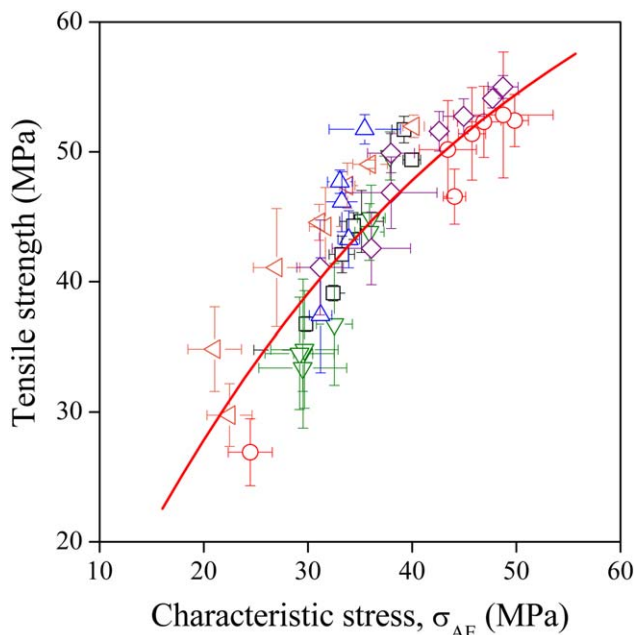
Figure 13. Correlation between the initiation stress of the dominating micromechanical deformation process and the ultimate tensile strength of the composites. Symbols are the same as in Figure 2. [Color figure can be viewed in the online issue, which is available at wileyonlinelibrary.com.]

REFERENCES

1. Markarian, J. *Plastics, Additives and Compounding* **2008**, *10*, 22.

2. Sawyer, D. *J. Macromol. Symp.* **2003**, *201*, 271.

3. Dorgan, J. R.; Lehermeier, H. J.; Palade, L.-I., Cicero, *J. Macromol. Symp.* **2001**, *175*, 55.

4. Auras, R.; Harte, B.; Selke, S. *Macromol. Biosci.* **2004**, *4*, 835.

5. Perego, G.; Cella, G. D. In Mechanical Properties, Auras, R., Lim, L.-T., Selke, S.; Tsuji, H., Eds.; John Wiley & Sons, Inc.; **2010**, p 141.

6. Lemmouchi, Y.; Murariu, M.; Dos Santos, A. M.; Amass, A. J.; Schacht, E.; Dubois, P. *Eur. Polym. J.* **2009**, *45*, 2839.

7. Martin, O.; Averous, L. *Polymer* **2001**, *42*, 6209.

8. Ljungberg, N.; Wesslen, B. *Polymer* **2003**, *44*, 7679.

9. Li, B.; Chen, S. C.; Qiu, Z. C.; Yang, Q. K. K.; Tang, S. P.; Yu, W. J.; Wang, Y. Z. *Polym. Bull.* **2008**, *61*, 139.

10. Ho, C. H.; Wang, C. H.; Lin, C. I.; Lee, Y. D. *Polymer* **2008**, *49*, 3902.

11. Södergard, A., Stolt, M. *Prog. Polym. Sci.* **2002**, *27*, 1123.

12. Gu, S. Y.; Zhang, K.; Ren, J.; Zhan, H. *Carbohydr. Polym.* **2008**, *74*, 79.

13. Rohman, G.; Laupretre, F.; Boileau, S.; Guerin, P.; Grande, D. *Polymer* **2007**, *48*, 7017.

14. Gorna, K.; Hund, M.; Vucak, M.; Grohn, F.; Wegner, G. *Mater. Sci. Eng. A-Struct. Mater. Prop. Microstruct. Process.* **2008**, *477*, 217.

15. Bleach, N. C.; Nazhat, S. N.; Tanner, K. E.; Kellomäki, M.; Törmälä, P. *Biomaterials* **2002**, *23*, 1579.

16. Bax, B.; Müssig, J. *Compos. Sci. Technol.* **2008**, *68*, 1601.

17. Murariu, M.; Ferreira, A. D.; Degee, P.; Alexandre, M.; Dubois, P. *Polymer* **2007**, *48*, 2613.

18. Kasuga, T.; Ota, Y.; Nogami, M.; Abe, Y. *Biomaterials* **2001**, *22*, 19.

19. Lin, P.-L.; Fang, H.-W.; Tseng, T.; Lee, W.-H. *Mater. Lett.* **2007**, *61*, 3009.

20. Nakayama, N.; Hayashi, T. *Polym. Degrad. Stab.* **2007**, *92*, 1255.

21. Luo, Y.-B.; Li, W.-D.; Wang, X.-L.; Xu, D.-Y.; Wang, Y.-Z. *Acta Mater.* **2009**, *57*, 3182.

22. Yuzay, I. E.; Auras, R.; Selke, S. *J. Appl. Polym. Sci.* **2010**, *115*, 2262.

23. Murariu, M.; Ferreira, A. D.; Pluta, M.; Bonnaud, L.; Alexandre, M.; Dubois, P. *Eur. Polym. J.* **2008**, *44*, 3842.

24. Kasuga, T.; Maeda, H.; Kato, K.; Nogami, M.; Hata, K.-I.; Ueda, M. *Biomaterials* **2003**, *24*, 3247.

25. Li, B.; Dong, F.-X.; Wang, X.-L.; Yang, J.; Wang, D.-Y.; Wang, Y.-Z. *Eur. Polym. J.* **2009**, *45*, 2996.

26. Chang, J.-H.; An, Y. U.; Cho, D.; Giannelis, E. P. *Polymer* **2003**, *44*, 3715.

27. Fukushima, K.; Tabuani, D.; Camino, G. *Mater. Sci. Eng. C* **2009**, *29*, 1433.

28. Fukushima, K.; Murariu, M.; Camino, G.; Dubois, P. *Polym. Degrad. Stab.* **2010**, *95*, 1063.

29. Murariu, M.; Dechief, A. L.; Bonnaud, L.; Paint, Y.; Gallos, A.; Fontaine, G.; Bourbigot, S.; Dubois, P. *Polym. Degrad. Stab.* **2010**, *95*, 889.

30. Cao, Y.; Feng, J.; Wu, P. *Carbon* **2010**, *48*, 3834.

31. Villmow, T.; Pötschke, P.; Pegel, S.; Häussler, L.; Kretzschmar, B. *Polymer* **2008**, *49*, 3500.

32. Kuan, C.-F.; Kuan, H.-C.; Ma, C.-C. M.; Chen, C.-H. *J. Phys. Chem. Solids* **2008**, *69*, 1395.

33. Wang, N.; Zhang, X. X.; Ma, X. F.; Fang, J. M. *Polym. Degrad. Stab.* **2008**, *93*, 1044.

34. Zhao, Y.-Q.; Lau, K.-T.; Kim, J.-k.; Xu, C.-L.; Zhao, D.-D.; Li, H.-L. *Compos. Part B* **2010**, *41*, 646.

35. Plackett, D.; Logstrup Andersen, T.; Batsberg Pedersen, W.; Nielsen, L. *Compos. Sci. Technol.* **2003**, *63*, 1287.

36. Huda, M. S.; Drzal, L. T.; Misra, M.; Mohanty, A. K. *J. Appl. Polym. Sci.* **2006**, *102*, 4856.

37. Huda, M. S.; Mohanty, A. K.; Drzal, L. T.; Schut, E.; Misra, M. *J. Mater. Sci.* **2005**, *40*, 4221.

38. Mathew, A. P.; Oksman, K.; Sain, M. *J. Appl. Polym. Sci.* **2005**, *97*, 2014.

39. Bledzki, A. K.; Jaszkiewicz, A.; Scherzer, D. *Compos. Part A: Appl. Sci. Manuf.* **2009**, *40*, 404.

40. Petinakis, E.; Yu, L.; Edward, G.; Dean, K.; Liu, H. S.; Scully, A. D. *J. Polym. Environ.* **2009**, *17*, 83.

41. Oksman, K.; Skrifvars, M.; Selin, J.-F. *Compos. Sci. Technol.* **2003**, *63*, 1317.

42. Way, C.; Wu, D.; Cram, D.; Dean, K.; and Palombo, E. *J. Polym. Environ.* **2013**, *21*, 54.

43. Zhang, Q.; Shi, L.; Nie, J.; Wang, H.; and Yang, D. *J. Appl. Polym. Sci.* **2012**, *125*, E526.

44. Quero, F.; Eichhorn, S.; Nogi, M.; Yano, H.; Lee, K.-Y.; Bismarck, A. *J. Polym. Environ.* **2012**, *20*, 916.

45. Faludi, G.; Dora, G.; Renner, K.; Móczó, J.; Pukánszky, B. *Carbohydr. Polym.* **2013**, *92*, 1767.

46. Faludi, G.; Hári, J.; Renner, K.; Móczó, J.; Pukánszky, B. *Compos. Sci. Technol.* **2013**, *77*, 67.

47. Molnár, K.; Móczó, J.; Murariu, M.; Dubois, P.; Pukánszky, B. *Exp. Polym. Lett.* **2009**, *3*, 49.

48. Dányádi, L.; Janecska, T.; Szabó, Z.; Nagy, G.; Móczó, J.; Pukánszky, B. *Compos. Sci. Technol.* **2007**, *67*, 2838.

49. Renner, K.; Móczó, J.; Pukánszky, B. *Compos. Sci. Technol.* **2009**, *69*, 1653.

50. Pukánszky, B. *Composites* **1990**, *21*, 255.

51. Renner, K.; Kenyó, C.; Móczó, J.; Pukánszky, B. *Compos. Pt. A-Appl. Sci. Manuf.* **2010**, *41*, 1653.

52. Dányádi, L.; Renner, K.; Móczó, J.; Pukánszky, B. *Polym. Eng. Sci.* **2007**, *47*, 1246.

53. Renner, K.; Yang, M. S.; Móczó, J.; Choi, H. J.; Pukánszky, B. *Eur. Polym. J.* **2005**, *41*, 2520.

54. Imre, B.; Keledi, G.; Renner, K.; Móczó, J.; Murariu, M.; Dubois, P. and Pukánszky, B. *Carbohydr. Polym.* **2012**, *89*, 759.

55. Fowkes, F. M. *J. Adhes. Sci. Technol.* **1987**, *1*, 7.

56. Vörös, G.; Fekete, E.; Pukánszky, B. *J. Adhes.* **1997**, *64*, 229.

57. Renner, K.; Móczó, J.; Vörös, G.; Pukánszky, B. *Eur. Polym. J.* **2010**, *46*, 2000.

58. Pukánszky, B.; Vörös, G. *Polym. Compos.* **1996**, *17*, 384.

59. Renner, K.; Móczó, J.; Suba, P.; Pukánszky, B. *Compos. Sci. Technol.* **2010**, *70*, 1141.